# Congestion Management through Optimal Allocation of FACTS Devices Using DigSILENT-Based DPSO Algorithm - A Real Case Study

*A. Bagheri[1*], A. Rabiee[1], S. Galvani[2] and F. Fallahi[3]*

*[1] Department of Electrical Engineering, Faculty of Engineering, University of Zanjan, Zanjan, Iran*
*[2] Faculty of Electrical and Computer Engineering, Urmia University, Urmia, Iran*
*[3] Planning and Research Deputy, Gilan Regional Electric Company, Iran*

**Abstract-** *Flexible AC Transmission Systems (FACTS) devices have shown satisfactory performance in alleviating the problems of electrical transmission systems. Optimal FACTS allocation problem, which includes finding optimal type and location of these devices, have been widely studied by researchers for improving variety of power system technical parameters. In this paper, a DIgSILENT-based Discrete Particle Swarm Optimization (DPSO) algorithm is employed to manage the power flow, alleviate the congestion, and improve the voltage profile in a real case study. The DPSO have been programmed in DPL environment of DIgSILENT software and applied to the power grid of Gilan Regional Electric Company (GilREC), located in north of Iran. The conducted approach is a user-friendly decision making tool for the engineers of power networks as it is executed in DIgSILENT software which is widely used in electric companies for the power system studies. The simulation results demonstrate the effectiveness of the presented method in improving technical parameters of the test system through several case studies.*

*Keyword:* FACTS devices allocation, Congestion management, SVC, PST, DPSO algorithm, DIgSILENT

## 1. INTRODUCTION

Transmission system is the most important intermediate environment between the load and generation in power grids. The proper operation and performance of this system in dynamic and steady-state conditions plays an important role in adequate and secure operation of the whole power system. Reduction of power loss and voltage drop in the path between generation and load has always been one of essential requirements of power system efficiency in steady-state conditions. On the other hand, the ability of power system in maintaining its stability during transient conditions following disturbances is the other feature of a reliable power system [1-3]. The two mentioned factors, i.e., keeping the acceptable voltage drop and dynamic and transient stability are the bounding constraints which prevent fully utilization of lines' and transformers' rated capacity. Also, as in restructured power systems, the consumers can choose their power suppliers and make contract with them, some transmission lines may be overloaded or congested [4]. If the congestion continues, the power grid is exposed to blackout. Also, if there is reactive power shortage, there may be voltage fluctuations leading to voltage collapse. In fact, one of

the major reasons for the voltage collapse is the limitation of reactive power in the network [5]. In this regard, several methods have been recommended and implemented by the researchers and engineers for the compensation of reactive power in order to improve the voltage conditions, reduce the power loss, and enhance the power system stability. The recent advancements in power electronic technologies have prepared new control devices for more efficient operation of existing power systems. In this respect, various control equipment named Flexible AC Transmission Systems (FACTS) have been designed and developed. Regarding the characteristics of FACTS devices, they can be considered as an adequate solution for the power flow control in the network to balance the loading of transmission and sub-transmission lines, which in turn, it results in power loss reduction, voltage profile improvement, damming the low frequency oscillations (LFOs), and increasing the stability margin. Up to now, several FACTS devices have been constructed and installed worldwide. Some of examples of them are given below:

1) South Africa (1995): SVC with the ratings of 275kV, [-300 +100] MVA (shown in Fig. 1).

2) France (2011): SVC with the ratings of 225kV, [-100 +100] MVA.

3) Nevada USA, PST with ratings of, 500kV, 60Hz, 650 MVA, ±24° (shown in Fig. 2).

Currently, in most of electric companies in Iran, there is no efficient control on the active power flow; also, the

voltage and reactive power are statically controlled using fixed capacitor banks and reactors. However, due to the seasonal and daily variations of loads, the static compensation may not have efficient capability in dynamic control of voltage and reactive power in different operating conditions. In this regard, the FACTS devices can be very useful in active and reactive power flow control of the system in all operating conditions, and they bring many benefits for the owners of the network. Based on the connection type, the FACTS devices fall in in three categories [6]. The first category includes devices that are connected in series with the power circuit, such as Thyristor-Controlled Series Capacitor (TCSC) and Static Synchronous Series Compensator (SSSC). The main role of this type of FACTS is the power flow control and damping of LFOs. The second type comprises the parallel devices such as Static Compensator (STATCOM) and Static VAr Compensator (SVC) which perform the task of voltage and reactive power control.
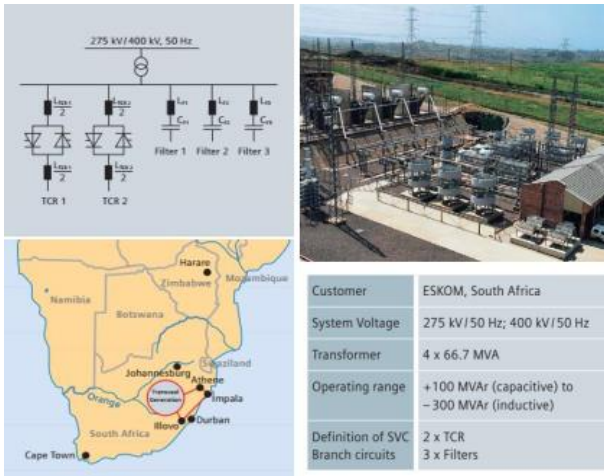


**Fig. 1. SVC project of South Africa**
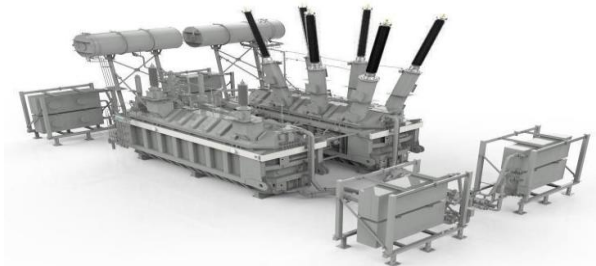


**Fig. 2. PST project of Nevada in USA**

The third category includes the equipment connected in series-parallel to simultaneously control the voltage and active power, such as Unified Power Flow Controller (UPFC) and Phase Shifting Transformer (PST). The aim of FACTS devices allocation includes finding the proper type, capacity, location, and parameter setting of these components. Several studies have been implemented for the FACTS allocation in transmission systems [7-19]. Ref. [7] employed SVC and TCSC to maximize the Available Transfer Capability (ATC) during normal and contingency situations. The ATC is calculated by the use of Continuation Power Flow (CPF) method considering

thermal limits and voltage profile. For the optimization purpose, the real-coded genetic algorithm (RGA) is used to determine the location and controlling parameters of SVC and TCSC. In Ref. [9], a novel global harmony search algorithm (NGHS) is utilized to find the optimal location and capacity of shunt reactive power compensators including capacitors, SVCs, and STATCOMs in transmission network; Modal analysis method is used for optimal placement of devices in the first sub-problem, and then, in the second sub-problem, NGHS algorithm is employed for optimization of the load flow. The objective function simultaneously considers enhancing of the voltage stability, improving the voltage profile, and reducing power losses while minimizing the total cost. Comparing the results of NGHS algorithm with those of improved harmony search algorithm (IHS) and particle swarm optimization (PSO) demonstrates the efficacy of the presented algorithm in terms of accuracy and convergence speed.

In Ref. [11], the type, size and location of FACTS devices, including TCSC and SVC, have been optimized by a Dedicated Improved Particle Swarm Optimization (DIPSO) algorithm. The objective function includes decreasing of overall costs of power generation and maximizing of profit. The main contribution of this paper is using Optimal Power Flow (OPF) and DIPSO algorithm to techno-economic analysis of the system for finding optimal operation. However, this work has not considered the contingency cases which may lead to voltage and power flow violations. In Ref. [12], a hybrid algorithm of Bacterial Foraging oriented by Particle Swarm Optimization (BF-PSO) combined with Optimal Power Flow (OPF) is used to obtain the best size and location of STATCOM in power systems. The main feature of this work is considering contingency analysis as lines outages may lead to infeasible solutions which can be settled by load shedding. The aim of the proposed algorithm is to mitigate overall power losses and costs and also, to prevent infeasible power flow solutions without undesired load-shedding. This paper has not employed the series FACTS devices for the sake of power flow management. A heuristic method based on Gravitational Search Algorithm (GSA) has been used in Ref. [14] for determining the optimal number and location of UPFC devices considering generation cost and power system losses. The proposed UPFC placement algorithm has been tested on several test systems, and the results are compared with other heuristic methods. Brainstorm optimization algorithm (BSOA) is employed in Ref. [15] to find optimal location and setting of SVC and TCSCs as FACTS devices. FACTS allocation problem is formulated as a multi-objective problem whose objectives are voltage profile enhancement and overload and loss minimization. The simulations have been carried out in MATLAB environment; the results verify that BSOA obtains better voltage profile and lower losses than PSO, GA, differential evolution (DE), simulated annealing (SA), hybrid of genetic algorithm and pattern search (GA-PS), backtracking search

algorithm (BSA), gravitational search algorithm (GSA) and asexual reproduction optimization (ARO) methods.

In Ref. [16], FACTS allocation problem has been formulated in MATLAB software as a sparsity-constrained OPF problem. An ADMM-IPM-STO algorithm, which combines the state-of-art algorithms in both sparse optimization and OPF, has been proposed to simultaneously determine the location, type, number, and setting values of FACTS devices. Ref. [17] proposes an approach for optimal allocation of multiple types of FACTS devices in power systems with wind generation under deregulated electricity market environment. The aim is to maximize the profit by minimizing investment and operating costs considering normal and contingency conditions. In fact, the objective includes maximizing social welfare and minimizing compensations paid for generation re-scheduling and load shedding. The problem is solved in two stages; in stage 1, optimal FACTS allocation is solved as the main problem and in stage 2, the optimal power flow is implemented as the sub-optimization using the MATPOWER version 4.1. Zhang et. al. [18] proposed a new approach for optimal locating of variable series reactor (VSR) in transmission network considering multiple operating states and contingencies. A reformulation technique transforms the original mixed integer non-linear programming model into mixed integer linear programming model. A two-phase decomposition algorithm is introduced to further relieve the computational burden and enable the planning model to be directly applied to practical large-scale systems. Ref. [19] presented a bi-level optimization model for optimal allocation of VSR and phase shifting transformer in the transmission system considering high penetration of wind power. The upper level problem seeks for minimizing the investment cost on FACTS devices, the cost of wind power curtailment, and possible load shedding. The lower level problem obtains the market clearing under different operating scenarios. A customized reformulation and decomposition algorithm is implemented to solve the proposed bi-level model. The simulations on the test system demonstrate the efficient performance of the proposed planning model and the important role of series FACTS for facilitating the integration of wind power. A shortcoming of both Ref. [18] and Ref. [19] is the use of DC power flow instead of AC model which ignores the power loss and reactive power, and also, the voltage constraints.

The review of literature reveals that the previous researches have implemented the optimization model in MATLAB or GAMS software packages. However, in real applications in electric companies, the network is usually simulated in DIgSILENT or PSSE (Power System Simulator for Engineering) environment. For the engineering application, one solution is that the network data is exported from DIgSILENT/PSSE to MATLAB/GAMS; then the optimization is fulfilled using mathematical or meta-heuristic algorithms, and finally, the results of optimization is returned to the source software. The other solution is to create a link between the source software (DIgSILENT/PSSE) and optimizing software (MATLAB/GAMS); the deficiency of this approach is that it makes the optimization procedure very time consuming, and it needs two software packages for installation; also, it may not be user-friendly for the engineers. The third solution is the use of optimization algorithm within the DIgSILENT or PSSE which is proposed in the current paper. The advantage of this approach is that there is no need for the data export. Also, it is possible to perform any steady state or transient analysis such as power flow, dynamic simulation, power quality analysis, short circuit analysis, etc., and link these analyzes with optimization algorithms within the software. Also, in power flow calculations, the results are obtained using AC model instead of approximate DC model.

In this paper, optimal allocation of SVC and PST, as two types of FACTS family, is implemented in order to alleviate the congestion and improve the voltage profile in Gilan Regional Electric Company as a real network in Iran. The objective function includes minimization of lines loading and buses' voltage deviation. Since the objective function is of non-linear nature and it is subjected to various constraints, and regarding the extent of the test system, the DPSO algorithm has been employed to optimize it. As the DIgSILENT is industrial software which is frequently employed by the engineers for the power system studies, and it is very accurate in power flow and other analyses, the PSO algorithm has been programmed in DPL (DIgSILENT Programming Language) environment of this software. The user can input the required information for the optimization, and extract the output results after convergence. The main features of this paper can be outlined as follows:

- Implementation of DPSO algorithm within the DIgSILENT software;
- User-friendly feature of the designed software;
- Generality of the designed software and its applicability to different networks;
- Complete AC modeling of system without any simplifications for the optimization purpose;
- Applying the proposed approach to a real network of Gilan electric company.

## 2. FACTS MODEL

For the reasons that will be stated later, among the FACTS devices, Static VAr Compensator (SVC) as a shunt device and Phase Shifting Transformer (PST) as a shunt-series device have been considered in this paper.

### 2.1. Model of SVC

SVC introduces variable shunt impedance in order to exchange capacitive or inductive current to maintain or control specific parameters of the electrical power system (typically bus voltage). SVC as shown in Fig. 3a is based on thyristors without the gate turn-off capability. It includes separate equipment for leading and lagging VArs: the thyristor-controlled or thyristor-

switched reactor (TCR/TSR) for absorbing reactive power and thyristor-switched capacitor (TSC) for supplying the reactive power. The V-I characteristic of SVC is depicted in Fig. 3b [6].

### 2.2. Model of PST

The phase shifting transformer (PST) is a specialized form of transformer used to control the active power flow in three phase electricity transmission networks. The term phase shifter is more generally used to indicate a device which can inject a voltage with a controllable phase angle and/or magnitude under no-load (off-load) and load (on-load) conditions.
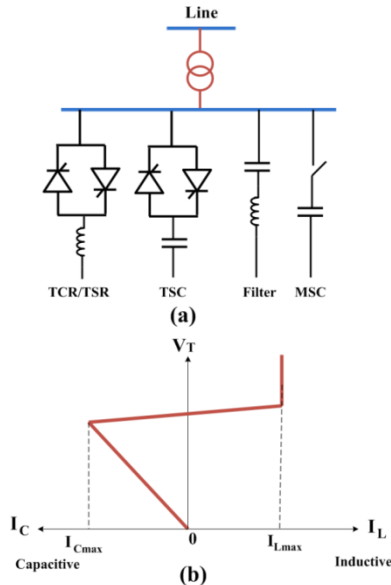


**Fig. 3. Structure of SVC, (a): Circuit diagram, (b): Voltage-Current characteristic**
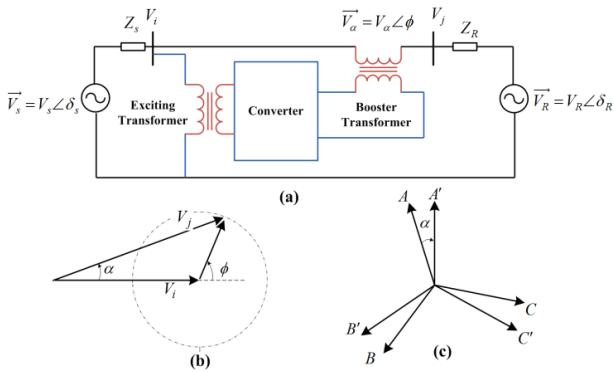


**Fig. 4: Phase shifting transformer (a) Circuit diagram, (b) phasor diagram (c) phase shift**

The main power circuitry of the phase shifting transformer as shown in Fig. 4a consists of: (1) the exciting transformer that provides input voltage to the phase shifter; (2) the series transformer that injects a controllable voltage $\vec{V_\alpha}$ in the transmission line; and (3) the converter or tap changer, which controls the magnitude and/or phase angle of the injected voltage.

A converter is used in the case of a power electronic based interface, and a tap changer is used in the case of a mechanical controlled phase shifting transformer [20]. The PST is used for power flow control in order to

relieve congestions in electrical grids. In Fig. 4a, the phase shifter has been installed on a transmission line between buses *i* and *j*. The sending and receiving ends of the transmission line are represented by voltage phasors $V_S$ and $V_R$, and corresponding impedances $Z_S$ and $Z_R$, respectively. Depending on the magnitude and phase angle of the injected voltage, $V_\alpha$, the magnitude and/or phase-angle of the system voltage, $V_j$, is varied (Fig. 4b and Fig. 4c). With a flexible phase shifting transformer, the control range achieved is a circle with center in the tip of the phasor $V_i$ and radius equal to the amplitude of $\vec{V_\alpha}$. The output voltage of the phase shifting transformer is controlled by varying the amplitude and angle of the phasor $\vec{V_\alpha}$, that is $V_\alpha$ and $\Phi$ [21]. The active power flow on the transmission line that incorporates a PST is given by Ref. [22]:

$$P = \frac{|V_S||V_R|}{X_{eq}} sin(\delta_S - \delta_R \pm \alpha)  \qquad (1)$$

Where, $Xeq$ is the net equivalent reactance of the line and the sources, whereas $\delta_S$ and $\delta_R$ are phase angles of the phasors $V_S$ and $V_R$, respectively. Based on equation (1), the angle $\alpha$ is the dominant variable for power flow control.

### 3. PROBLEM FORMULATION

The optimal FACTS allocation is an optimization problem which can be described by objective function and constraints as the following.

### 3.1. Objective function

The considered objective function ($f_{total}$) is a two-objective one combined as a single-objective function using the weighting factors as (2). This objective aims at:

- Minimizing the loading of transmission and sub-transmission lines in normal and contingency operating conditions;
- Improving the voltage profile of transmission and sub-transmission substations in normal and contingency operating conditions.

In Eq.2 $\bar{f}_{Loading}$ and $\bar{f}_{Voltage}$ respectively are the objective functions of loading and voltage profile which have been normalized as (3)-(5).

$$f_{total} = w_1 \bar{f}_{Loading} + w_2 \bar{f}_{Voltage}  \qquad (2)$$

$$f_{Loading} = \sum_{b \in \Omega_L} \sum_{\forall \ell} \sum_{\forall c} \left( \alpha_{b,\ell,c} \times \mu_{b,\ell,c} \times S_{b,\ell,c} \right) + \sum_{t \in \Omega_T} \sum_{\forall \ell} \sum_{\forall c} \left( \gamma_{t,\ell,c} \times S_{t,\ell,c} \right)  \qquad (3)$$

$$\bar{f}_{Loading} = \frac{f_{Loading}}{f_{L0}}  \qquad (4)$$

$$f_{Voltage} = \sum_{i \in \Omega_B} \sum_{\forall \ell} \sum_{\forall c} \beta_{i,\ell,c} |V_{i,\ell,c} - 1|  \qquad (5)$$

$$\bar{f}_{Voltage} = \frac{f_{Voltage}}{f_{V0}}  \qquad (6)$$

Where:

| $i$ | Index of bus number (transmission and sub-transmission) |
|---|---|
| $b$ | Index of line number |
| $t$ | Index of HV/MV transformer number |
| $\ell$ | Index of load level (peak and off-peak) |
| $c$ | Index of contingency number ($c_0$ for the base case, and $c_1$, $c_2$, ...for contingencies) |
| $f_{total}$ | Total objective function |
| $f_{Loading}$ | Loading of transmission and sub-transmission lines |
| $\bar{f}_{Loading}$ | Normalized value of loading of transmission and sub-transmission lines |
| $f_{L0}$ | Loading of transmission and sub-transmission lines in base case (before optimization) |
| $f_{voltage}$ | Voltage deviation of buses |
| $\bar{f}_{Voltage}$ | Normalized value of voltage deviation of buses |
| $f_{V0}$ | Voltage deviation of buses in base case (before optimization) |
| $\alpha_{b,\ell,c}$ | Penalty factor for loading violation of transmission line $b$ in load level $l$, and contingency $c$ |
| $\mu_b$ | Weighting factor for the voltage level importance of transmission line $b$ |
| $\gamma_{t,\ell,c}$ | Penalty factor for loading violation of transformer $t$ in load level $l$, and contingency $c$ |
| $\beta_{i,\ell,c}$ | Penalty factor for voltage violation of substation $i$ in load level $l$, and contingency $c$ |
| $w_1, w_2$ | Weighting factors of objective functions |
| $\Omega_L$ | Set of transmission lines |
| $\Omega_B$ | Set of transmission and sub-transmission substations |
| $\Omega_T$ | Set of HV/MV transformers |
| $S_{b,\ell,c}$ | Loading of line $b$ in load level $l$, and contingency $c$ |
| $S_{t,\ell,c}$ | Loading of HV/MV transformer $t$ in load level $l$, and contingency $c$ |
| $V_{i,\ell,c}$ | Voltage of transmission/sub-transmission substation $i$ in load level $l$, and contingency $c$ |

In the objective function, the parameter $\mu$, which is defined as the weighting factor for the voltage level of transmission line, shows the importance of lines in terms of the objective function. The lines of Gilan network are in four voltage levels including 400kV, 230kV, 132kV, and 63kV. If all lines have equal importance from the viewpoint of electric company, the parameter $\mu$ will be equal for all voltage levels. For the electric companies, normally the lines with higher voltage levels are more important. For this aim, the

optimization algorithm can consider more importance for these lines compared to lower voltage levels by adjusting the value of $\mu$. In total, this parameter gives more flexibility for the system owner in controlling the loading importance of his networks equipment. In this paper, the importance of higher voltage levels is considered more than that for lower voltage levels.

### 3.2. Constraints

In the proposed problem, the AC model has been used for power flow calculations. Therefore, the constraints governing the problem are as (7)-(13).

$$P_{G_i,\ell,c} - P_{D_i,\ell,c} = V_{i,\ell,c} \sum_{j \in \Omega_i} V_{j,\ell,c} Y_{ij,c}$$
$$\cos\left(\delta_{i,\ell,c} - \delta_{j,\ell,c} - \theta_{ij,c} + \phi_{ij,\ell,c}\right) \forall i \in \Omega_B \ , \ \forall \ell, \ \forall c \quad (7)$$

$$Q_{G_i,\ell,c} - Q_{G_i,\ell,c} + Q_{i,\ell,c}^{SVC} = V_{i,\ell,c} \sum_{j \in \Omega_i} V_{j,\ell,c} Y_{ij,c}$$
$$\sin\left(\delta_{i,\ell,c} - \delta_{j,\ell,c} - \theta_{ij,c} + \phi_{ij,\ell,c}\right); \ \forall i \in \Omega_B \ , \ \forall \ell, \ \forall c \quad (8)$$

$$P_{G_i}^{\min} \leq P_{G_i,\ell,c} \leq P_{G_i}^{\max} \ ; \ \forall i \in \Omega_B^G \ , \ \forall \ell, \ \forall c \quad (9)$$

$$Q_{G_i}^{\min} \leq Q_{G_i,\ell,c} \leq Q_{G_i}^{\max} \ ; \ \forall i \in \Omega_B^G \ , \ \forall \ell, \ \forall c \quad (10)$$

$$Q_i^{SVC,\min} \leq Q_{i,\ell,c}^{SVC} \leq Q_i^{SVC,\max} \ ; \ \forall i \in \Omega_B^{SVC} \ , \ \forall \ell, \ \forall c \quad (11)$$

$$V_{i,\ell,c} = V_{i,\ell}^{spc} \ ; \ \forall i \in \Omega_B^{SVC} \ , \ \forall \ell, \ \forall c \quad (12)$$

$$\phi_{ij}^{\min} \leq \phi_{ij,\ell,c} \leq \phi_{ij}^{\max} \ ; \ \forall ij \in \Omega_L^{PS} \ , \ \forall \ell, \ \forall c \quad (13)$$

Where,

| $\Omega_B^{SVC}$ | Set of candidate buses for SVC installation |
|---|---|
| $\Omega_L^{PST}$ | Set of candidate transmission lines for PST installation |
| $\Omega_B^G$ | Set of power generating buses |
| $V_{i,\ell}^{spc}$ | Reference voltage of sub-transmission substations equipped with SVC in loading level $l$ |
| $(P/Q)_{G_i,\ell,c}$ | Active/reactive power generation at bus $i$, in load level $l$, and contingency $c$ |
| $(P/Q)_{D_i,\ell,c}$ | Active/reactive power demand at bus $i$, in load level $l$, and contingency $c$ |
| $\delta_{i,\ell,c}$ | Voltage angle of transmission/sub-transmission substation $i$ in load level $l$, and contingency $c$ |
| $Y_{ij,c} \angle \theta_{ij,c}$ | ij-th element of system admittance matrix. |
| $\phi_{ij,\ell,c}$ | Voltage angle deviation by the PST between nodes $i$ and $j$, in load level $l$, and contingency $c$ |
| $Q_{i,\ell,c}^{SVC}$ | Injected reactive power of SVC installed on bus $i$ in load level $l$, and contingency $c$ |

The relations (7) and (8) are the active and reactive power balance in buses in the presence of SVC and PST; Generators' active and reactive power limit are expressed by (9) and (10); relation (11) denotes the limitation of SVC units' reactive power injection/absorption. The reference voltage of sub-transmission substations on which the SVC has been installed is represented by (12). This reference value can

be selected by the user. Finally, (13) declares the range of tap position (phase angle) for the PST units.

## 4. PARTICLE SWARM OPTIMIZATION

Considering the objective function and its constraints, the considered problem is a non-linear optimization which requires appropriate solution methodologies. Many of practical problems like the one in this paper are so complicated that the mathematical methods are not able to solve them. In this regard, the heuristic and meta-heuristic (known also as intelligent) approaches are usually exploited. Various meta-heuristic algorithms have been developed and applied to large extent of power system operation and planning problems; such as genetic algorithm (GA), simulated annealing (SA) [15], differential evolution (DE) [15], particle swarm optimization (PSO), harmony search algorithm (HSA) [9, 23], chemical reaction optimization algorithm (CROA) [13], gravitational search algorithm (GSA) [14], brainstorm optimization algorithm (BSOA) [15], and etc. As the performance of PSO algorithm has been proved in literature, it will be employed in this paper for the optimization purpose, and it will be described in details subsequently.   PSO, as a meta-heuristic method, was originally introduced in 1995 by Eberhart and Kennedy [24]. PSO falls in the category of population-based algorithms, and it has been inspired from the social behavior of animals like fishes and birds as the particles. The behavior of particles is based on coordination of their movement velocity and position with the neighbor particles [25, 26]. The advantage of PSO over the other algorithms is its simple and fast calculations and fewer parameters to be tuned. In PSO, like the other intelligent algorithms, an objective function is considered, and a set of candidate solutions are expressed as the position of particles. The particles move in a *D*-dimensional search space, and they exchange their experience with the neighbors to update their velocity and position aiming at finding the food position as the optimal solution of the algorithm. The detailed description of PSO can be found in references [24-26]. If the best personal experience and the best experience among the whole particles are represented respectively by *pbest* and *gbest*, the equations for the velocity and position can be expressed as Eq. (14) and Eq. (15):

$$v_{id}(t+1) = fix\{ \omega v_{id}(t) + c_1 rand_1( p_{id}(t) - x_{id}(t)) + c_2 rand_2( g_d(t) - x_{id}(t))\} \tag{14}$$

$$x_{id}(t+1) = x_{id}(t) + v_{id}(t+1) \tag{15}$$

$$\omega = \frac{iter^{max} - iter}{iter^{max}} \tag{16}$$

In Eq. (14), $c_1$ and $c_2$ are the acceleration coefficients; $r_1$ and $r_2$ are random numbers uniformly distributed in range [0,1]; $\omega$ is the inertia coefficient which is linearly decreased as a function of iteration number (iter) as Eq. (16) [27]; The term *fix{}* in Eq. (14) applies when using

discrete type of PSO algorithm (DPSO), and it rounds the position to the nearest integer value. As the decision variables in this paper have discrete nature, the DPSO algorithm is employed here.

## 5. NUMERICAL STUDY

### 5.1. Introducing the case study: Gilan Regional Electric Company

Gilan Regional Electric Company (GilREC), as shown in Fig. 5, is located in north of Iran near the Caspian Sea [28]. Due to the security concerns, the authors are not allowed to present the name of substations in Fig. 5. Instead, the substations have been illustrated by short names (S1, S2, … for the transmission substations, and G1, G2, … for the power plants). GilREC is neighbor to four other electric companies in Iran, and also to the Azarbaijan country's grid; from the south, it is connected to Tehran and Zanjan networks; from the east, it is linked to Mazandaran electric company; and from the west, it is neighbor to Azarbaijan network and Azarbaijan country's power grid. The total peak load of this network in 2018 was 1540MW, and the average annual load growth rate has been 8% during the last 10 years. There are four central power plants within the governed area of this network (shown by G1, G2, G3 and G4 in Fig. 5) including combined-cycle power plant of Gilan with the nominal generation capacity of 1305MW, steam power plant of Loshan with the capacity of 240MW, steam-gas power plant of Paresar with the capacity of 968MW, and hydro power plant of Sefidrood with the capacity of 55MW. The loads within the Gilan network are supplied by the mentioned power plants and also through the transmission lines linking the Gilan network to its neighboring grids. The number of 400/230kV, 230/63kV, 132/20kV, and 63/20kV substations in GilREC are 1, 12, 2, and 33, respectively. Also, the length of 400kV, 230kV, 132kV, and 63kV lines respectively are 273, 1119.5, 87.93, and 1395.9 kilometers. Regarding the location of GilREC and its connection with the other electric companies, management of the power flow in this network is very important both from technical viewpoints (such as power loss, voltage drop, and stability in contingency conditions) and power market and available transmission capacity considerations. Considering the load and geographical dimensions, Gilan's network is a compact grid with high load density. The major problem in this network is the voltage drop and reactive power shortage of sub-transmission substations in peak load conditions. In this regard, installation of shunt FACTS devices would be useful. On the hand, in off-peak conditions, as the generated power inside the Gilan grid is much higher than the off-peak load, the transmission lines between this grid and the neighboring networks are congested. As a consequence of congestion occurrence, it is required to turn off some generating units; this results in generation block and encountering economic damages in power market.
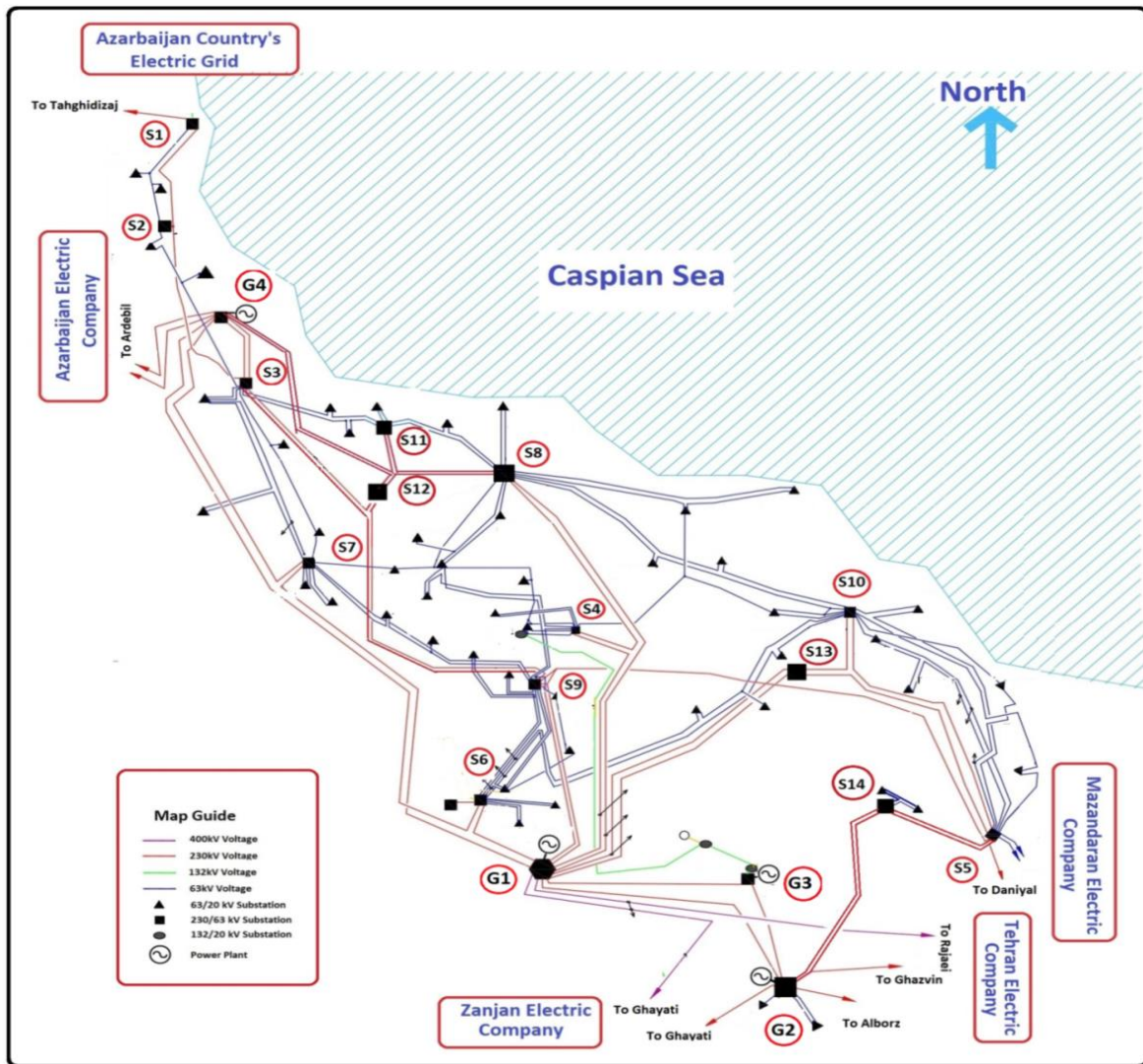
**Fig. 5. Geographical schematic of Gilan Regional Electric Company [28]**
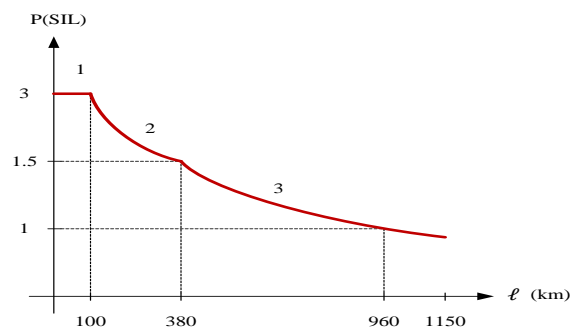


**Fig. 6. Load-ability curve of a typical transmission line in 50Hz**

To settle this problem, the use of appropriate types of series or series-shunt FACTS devices would be helpful. For the aim of the FACTS allocation, the planning horizon is considered to be the year of 2026. In this year, the total load of system in the peak and off-peak conditions will be 2535MW and 1244MW, respectively, which shows 65% increase compared to the base year (2018). Considering the load growth, to adequately

supply the loads, some substations and transmission lines have been decided to be installed until 2026. On this basis, in year 2026, Gilan network will include 14 transmission substations with the rated voltage of 230kV/63kV. These substations are presented in Table 1. The 63kV sides of these substations have been regarded as the candidate buses for the SVC installation. Also, all the 230kV lines, including 43 transmission

lines, are considered as candidates for the installation of PST. In order to evaluate the use of FACTS devices, four worst-case conditions are considered based on the experience of the GilREC's experts. In these four conditions, as Table 2, it is supposed that the Gilan network can exchange the power only with one of the neighboring networks. In the other words, in each scenario, a substation in the related neighboring network is considered as the slack (reference) bus. In addition to the normal conditions of peak and off-peak load, the behavior of network should also be investigated in the contingency cases. For this aim, a contingency analysis is performed in DIgSILENT to diagnose the critical line outages in which there is severe voltage drops in the substations or high loadings in transmission and sub-transmission lines. These contingencies have been listed in Table 3. In this table, the lines are described by their ending substations shown by short names. As mentioned before, among the FACTS devices, in this paper, SVC and PST are employed to resolve the problems of Gilan network. The reason for choosing SVC and PST among the FACTS family can be stated as follows:

The power flowing through a transmission line can be constrained by several factors. Fig. 6 shows the load-ability curve of transmission lines in 50Hz frequency [29]. This curve shows the transmitted power in terms of SIL (surge impedance loading) versus the length of line. In this figure, area 1 is related to thermal limitation range (for the short lines), area 2 corresponds to voltage drop constraint (for the medium-length lines), and area 3 is due to the stability margin (for long lines). In the Gilan network, there are no long lines so that the average lengths of 230kV and 63kV lines are 40km and 11km, respectively. This shows that the problem of lines in this network is related to area 1 of Fig. 6 (i.e., in which the transmission lines reach to their thermal limit). The devices such as TCSC and SSSC are two familiar types of series FACTS devices which are employed to reduce the line's series impedance when the loading limitation is related to stability constraint. But, Gilan lines loading limitation is due to reaching to their thermal capacity. On the other side, Gilan transmission and sub-transmission systems is a highly meshed network, such that there are several 230kV and 63kV loops (or rings). For such a network, in order to control the active power flow (for the sake of congestion management and removing the generation block), it is required to use active power control devices such as PSTs. The power flowing through a transmission line can be constrained by several factors. Fig. 6 shows the load-ability curve of transmission lines in 50Hz frequency [29]. This curve shows the transmitted power in terms of SIL (surge impedance loading) versus the length of line. In this figure, area 1 is related to thermal limitation range (for the short lines), area 2 corresponds to voltage drop constraint (for the medium-length lines), and area 3 is due to the stability margin (for long lines). In the Gilan network, there are no long lines so that the average lengths of 230kV and 63kV lines are 40km and

11km, respectively. This shows that the problem of lines in this network is related to area 1 of Fig. 6 (i.e., in which the transmission lines reach to their thermal limit). The devices such as TCSC and SSSC are two familiar types of series FACTS devices which are employed to reduce the line's series impedance when the loading limitation is related to stability constraint. But, Gilan lines loading limitation is due to reaching to their thermal capacity. On the other side, Gilan transmission and sub-transmission systems is a highly meshed network, such that there are several 230kV and 63kV loops (or rings). For such a network, in order to control the active power flow (for the sake of congestion management and removing the generation block), it is required to use active power control devices such as PSTs.

**Table 1. Characteristics of candidate substations for SVC installation**

| Substation name | | Rated Voltage | Capacity (MVA) |
|---|---|---|---|
| S1 | 1 | 230kV/63kV | 2×40 |
| S2 | 2 | 230kV/63kV | 2×90 |
| S3 | 3 | 230kV/63kV | 2×125 |
| S4 | 4 | 230kV/63kV | 3×160 |
| S5 | 5 | 230kV/63kV | 2×125 |
| S6 | 6 | 230kV/63kV | 3×160 |
| S7 | 7 | 230kV/63kV | 2×160 |
| S8 | 8 | 230kV/63kV | 2×160 |
| S9 | 9 | 230kV/132kV/63kV | 2×160+2×50 |
| S10 | 10 | 230kV/63kV | 2×125 |
| S11 | 11 | 230kV/63kV | 2×160 |
| S12 | 12 | 230kV/63kV | 3×160 |
| S13 | 13 | 230kV/63kV | 3×160 |
| S14 | 14 | 230kV/63kV | 2×40 |

**Table 2. Worst-case operation scenarios in peak and off-peak conditions**

| Scenario No. | Description | |
|---|---|---|
| | Power exchanging neighboring network | Location of neighboring network |
| 1 | 400kV bus of Rajaei Power plant in Tehran grid | South |
| 2 | 230kV bus of Ghayati substation in Zanjan grid | South |
| 3 | 230kV substation of Daniyal substation in Mazandaran grid | East |
| 4 | 230kV bus of Ardebil substation in Azarbaijan grid | West |

On the other hand, due to network's highly loaded lines and substations, especially in peak loading condition, and also, due to improper flow of reactive power which brings about high voltage drop and power losses, the use of shunt compensators in sub-transmission level (i.e. 63kV) looks inevitable. With appropriate reactive power compensation, the voltage profile becomes flat, which in turns, it reduces the reactive power flow and the loading of lines and transformers. Regarding the change of operation conditions (such as hourly and daily load variations), it is better to compensate the reactive power dynamically using the FACTS devices like SVC instead of conventional compensators such as shunt capacitor

banks. Although other shunt devices such as STATCOM, or series-shunt devices like UPFC can be employed for settling the problems of Gilan network, but, such devices have higher costs compared to SVC and PST, and also their control systems are much more complicated. With regard to these explanations, the PST has been used for the active power flow control, and SVC is employed as the shunt reactive compensator.

**Table 3. Critical contingencies considered in FACTS allocation in Gilan Network**

| Scenario No. | Critical contingencies in peak (From -To) | Critical contingencies in off-peak (From -To) |
|---|---|---|
| 1 | G1-S6<br>G1-S4<br>G1-S7<br>G4-S3<br>S1-S2<br>S3-S2<br>TaghiDizaj-S1 | S1-S2<br>S3-S2 |
| 2 | G1-S6<br>G1-S4<br>G1-S7<br>G4-S3<br>TaghiDizaj-S1 | G1-G2<br>G1-G3<br>S5-S14<br>G2-S14<br>G3-G2 |
| 3 | G1-S6<br>G1-S4<br>G1-S7<br>G4-S3<br>TaghiDizaj-S1 | G1-S10<br>G1-S13<br>S13-S5<br>S10-S5 |
| 4 | G1-S6<br>G1-S4<br>G4-S3<br>TaghiDizaj-S1 | G1-S6<br>G1-S8<br>G1-S7<br>G1-S4 |

## 5.2. Applying DPSO to FACTS devices allocation in GilREC

For encoding the decision variables of the problem, the structure of a typical particle has been depicted in Fig. 7. As seen in Fig. 7, the proposed particle is composed of different parts. The first and second parts represent the location of SVC and PST units, respectively. For the typical particle of Fig. 7, the first SVC is installed on bus 3, and the second PST is installed on line 37. The parts 3, 4, and 5 (which are repeated for the number of PST units) show the tap position of PSTs in normal and contingency conditions of peak and off-peak load levels; for example, the tap position of the first PST in normal operation of peak condition is +2, and it is -5 for the second contingency in off-peak condition.

## 5.3. Solving the FACTS allocation problem in GilREC using DPSO

The structure of the particle was presented in Fig. 7. For calculating the objective function, the particle must be decoded. For the codification purpose, in each of four operation scenarios, considering the values dedicated for each particle, the location of SVCs and PSTs, and also, the tap position of PSTs in peak and off-peak conditions are determined. By placing the SVCs and PSTs in the related locations in the network, the power flow calculation is performed for four states: (a) normal condition of peak load, (b) normal condition of off-peak load, (c) contingency condition of peak load, and (d) contingency condition of off-peak load. In all of the four states, it is aimed to resolve the congestion in transmission lines such that no generation is blocked within the network. By performing the power flow, the loading of the lines and substations, and also, the voltage of the substations are obtained; and on this basis, the objective function is calculated. The procedure of problem optimization can be depicted in Fig. 8. This procedure is accomplished for the four scenarios defined in Table 2; and at the end, the best configuration which suits for all four scenarios is chosen. For the optimization purpose, the values of PSO parameters is considered as $c_1=1$ and $c_2=3$; also the number of particles has been set to 15. In the flowchart of Fig. 8, the nominal capacity of each PST is calculated as (17)-(19) based on its tap range and the capacity of line on which the PST is installed;

$$S_{PST} = 2 \times sin(\alpha) \times S_{Line} \qquad (MVA) \qquad (17)$$

$$\alpha = 2.5° \times Tap^{max} \qquad (18)$$

$$S_{Line} = \sqrt{3} \times (230)^{kV} \times (I_{Line}^{max})^{kA} \qquad (MVA) \qquad (19)$$

where, $Tap^{max}$ is the absolute value of maximum/minimum tap position of PST in peak, off-peak, and contingency conditions which is determined by the PSO after the algorithm's convergence; also, $I_{Line}^{max}$ is the transmission line's thermal capacity in kA. The phase shift of each tap is also considered as 2.5 degree.
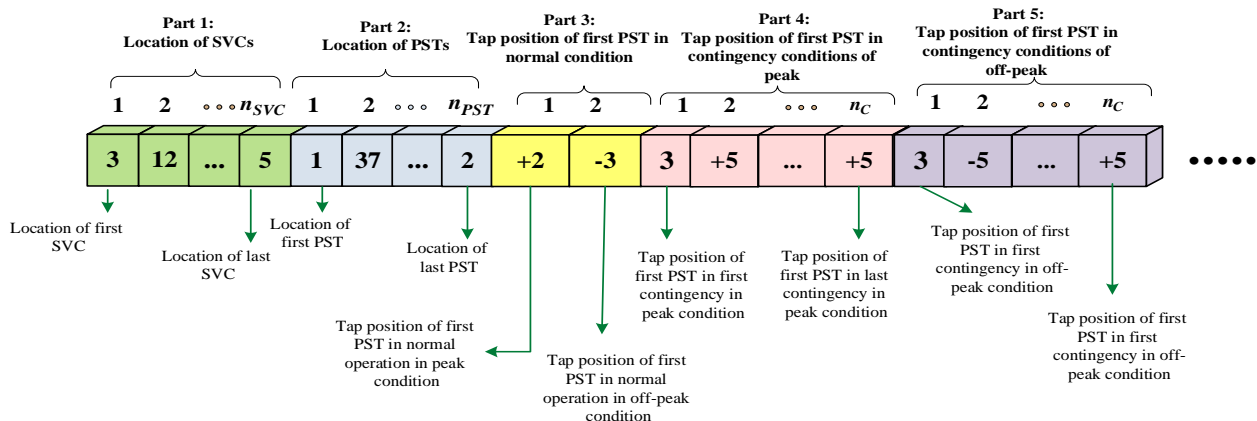


**Fig. 7. Structure of a typical particle in DPSO for FACTS allocation**
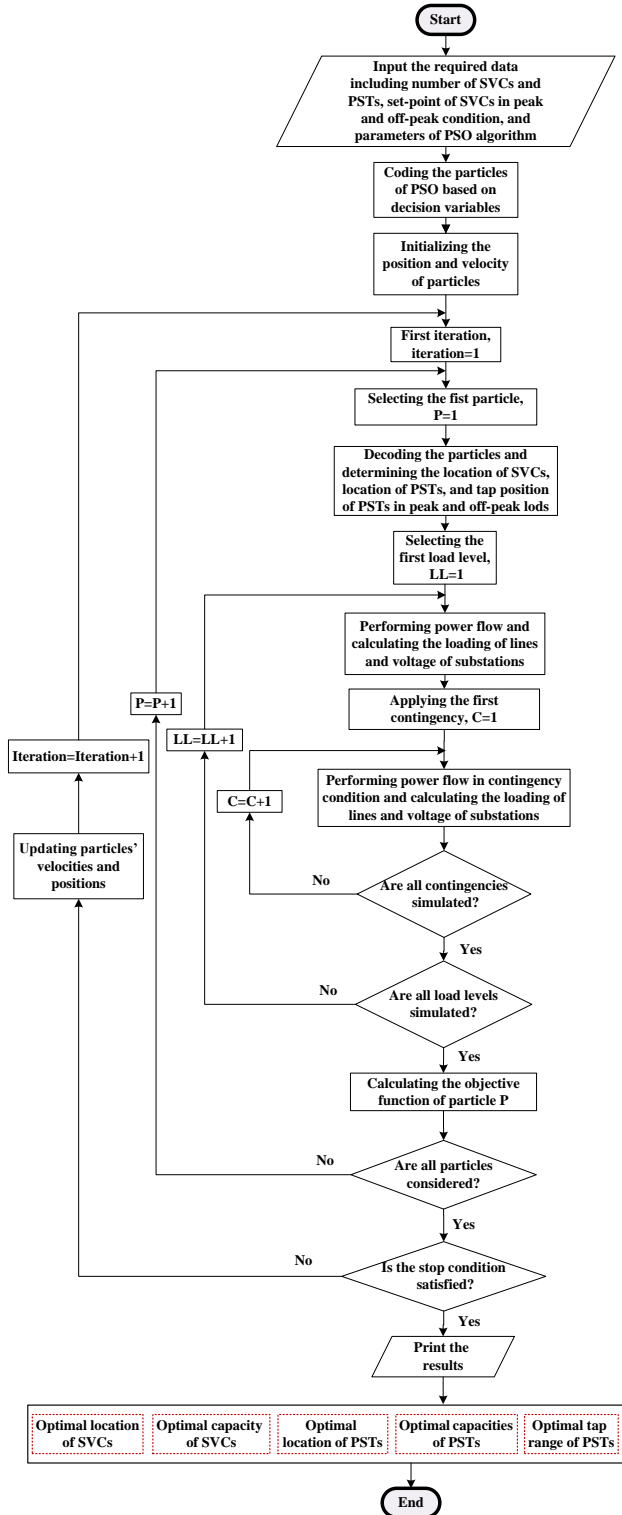
**Fig. 8. Optimization procedure of FACTS devices allocation using DPSO**

## 5.4. Simulation results

### 5.4.1. Scenario1

In this scenario, the regional network of Gilan exchanges the power with one of its south neighboring grids, i.e., Tehran regional electric company (TREC) through 400kV substation of Rajaei power plant located

in TREC. The results of optimization using DPSO are given in Tables 4 to 8. Table 4 shows the location and tap position of PSTs in normal and contingency conditions. Based on Eq. (17) and according to tapping range obtained from Table 4, the capacity of PSTs can be calculated as Table 5. Also, Table 6 represents the optimal location and injected reactive power of SVCs; based on Table 6 and considering the maximum injected reactive power of SVCs, their capacity will be determined as Table 7. To study the effect of FACTS devices on the network, the voltage of transmission substations with and without the use of FACTS devices are presented in Table 8. As seen, the voltages of substations have been improved in the presence of SVC and PST. Also, the voltage of buses on which the SVC has been installed is adjusted to 1 p.u. In addition, the voltage profile of 63kV and 132kV buses of sub-transmission substations have been illustrated in Fig. 9 for scenario 1. It can be observed that the voltage profile has been significantly improved, and the voltage magnitudes have become closer to 1p.u. The transmission lines' loading as the percentage of their nominal capacity are depicted in Fig. 10 for the peak and off-peak conditions of scenario 1. It is observed that by the FACTS installation, some high loadings have been decreased, and some low loadings are increased such that the lines' loading have been balanced after the compensation.
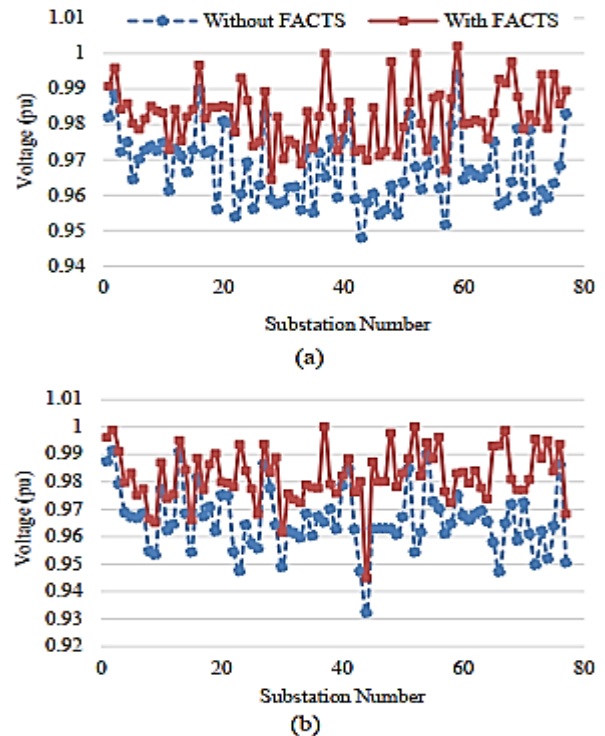


**Fig. 9. Voltage magnitude of sub-transmission level buses before and after installation of FACTS devices for scenario 1 (a): peak (b): off-peak**

**Table 4. Optimal location and tap position of installed PSTs in scenario 1**

| PST No. | Line on which the PST is installed | Tap Position | | | | | | | | | | |
|---|---|---|---|---|---|---|---|---|---|---|---|---|
| | | Normal Operation | | Contingency Operation (Contingency Number) | | | | | | | | |
| | | Peak | Off-peak | Peak | | | | | | | Off-peak | |
| | | | | 1 | 2 | 3 | 4 | 5 | 6 | 7 | 1 | 2 |
| 1 | S6-G4 | +2 | +3 | +3 | 0 | -4 | +2 | +2 | +1 | +3 | -2 | 0 |
| 2 | S3-S12 | 0 | +2 | 0 | 0 | -1 | -2 | -1 | +1 | 0 | +1 | +1 |

**Table 5. Characteristics of installed PSTs in scenario 1**

| PST No. | Capacity of PST (MVA) | Tap range (phase shift of each tap is 2.5$^O$ ) |
|---|---|---|
| 1 | 134 | ±4 |
| 2 | 67.3 | ±2 |

**Table 6. Optimal location and injected reactive power of installed SVCs in scenario 1**

| SVC No. | Substation on which the SVC is installed | Injected Reactive Power (MVAr) | | | | | | | | | | |
|---|---|---|---|---|---|---|---|---|---|---|---|---|
| | | Normal Operation | | Contingency Operation (Contingency Number) | | | | | | | | |
| | | Peak | Off-peak | Peak | | | | | | | Off-peak | |
| | | | | 1 | 2 | 3 | 4 | 5 | 6 | 7 | 1 | 2 |
| 1 | S7 | 62.1 | 108.9 | 57.2 | 115.8 | 69.9 | 64.8 | 63.2 | 62.6 | 65.4 | 109 | 108.6 |
| 2 | S6 | 129.9 | 132 | 207.6 | 118.9 | 142.9 | 132.4 | 130.6 | 130.9 | 132.6 | 132.4 | 132.3 |

**Table 7: Characteristics of installed SVCs in scenario 1**

| SVC No. | Capacity of SVC (MVAr) |
|---|---|
| 1 | 207.6 |
| 2 | 67.3 |

### 5.3.2. Scenario 2

In this scenario, the regional network of Gilan exchanges the power with Zanjan regional electric company (ZREC) through 230kV bus of 400/230/63kV Ghayati substation located in ZREC. The results of this scenario are obtained as Table 8, Tables 9-12, and Figs. 11 to 12. Improvement of the network's technical parameters is clearly seen in Figs. 11 and 12. In the peak condition, the generation of power plants is almost equal to the network' load, and hence, there is negligible power exchange with the neighboring grids. However, in the off-peak condition, as the generation is almost 1200MW more than the load, the surplus power is exchanged with the ZREC, and the transmission lines of Gilan network toward the south part are congested. This condition has been shown in Fig. 13a. As seen, the lines outgoing from G1 power plant toward G2 power plant have high loadings, and the line between G1 and G2 substations (named '3' in Fig.12.b) is highly overloaded by about 143%. After the placement of PST and SVC with the characteristics of Tables 9 to 12, the congestion has been resolved so that the loading of line G1-G2 is reduced from 142.7% to 86.2%.

According to Fig. 13b, the presence of two PSTs along with proper tap adjustment of them has resulted in the change of power flow, so that the power is transmitted to the substations located in eastern part of the network and returns to G2 substation from the direction shown in Fig. 13b; this leads to removing the congestion and lines' overload. In this way, the congestion is alleviated in the network and no generation is blocked, and no economic loss is imposed to the network owner.

### 5.3.3. Scenario 3

In this scenario, the surplus generated power of Gilan network is exchanged with Mazandaran regional electric company (MaREC) through 230kV bus of 230/63kV Danyal substation located in MaREC. The results of this scenario are presented in Table 8, Tables 13-16 and Figs. 14 to 15.

### 5.3.4. Scenario 4

In this scenario, the regional network of Gilan exchanges the power with Azarbaijan regional electric company (AZREC) through 230kV bus of 230/63kV Ardebil substation located in AZREC. The results of this scenario are presented in Table 8, Tables 17-20 and Figs. 16 to 17.

**Table 8. Voltage magnitude of HV substations before and after installation of FACTS devices for peak and off-peak conditions**

| Substation Name | Voltage level (kV) | Voltage Magnitude (Pu.) | | | | | | | | | |
|---|---|---|---|---|---|---|---|---|---|---|---|
| | | Peak | | | | | Off-Peak | | | | |
| | | Before Installation | After Installation | | | | Before Installation | After Installation | | | |
| | | | Sc. 1 | Sc. 2 | Sc. 3 | Sc. 4 | | Sc. 1 | Sc. 2 | Sc. 3 | Sc. 4 |
| G1 | 400 | 1.0037 | 1.0084 | 1.0084 | 1.0087 | 1.0086 | 0.9734 | 0.9892 | 1.0017 | 1.0051 | 1.0061 |
| | 230 | 0.9974 | 1.0056 | 1.0053 | 1.0057 | 1.0056 | 0.9848 | 0.994 | 0.9963 | 1.0022 | 1.0041 |
| G2 | 230 | 0.9987 | 1.0019 | 1.0016 | 1.0019 | 1.0019 | 0.9959 | 0.9984 | 0.935 | 0.9964 | 1.0027 |
| | 63 | 0.9987 | 0.9863 | 0.9869 | 0.9862 | 0.9864 | 0.9800 | 0.9873 | 0.9235 | 0.9856 | 0.9916 |
| G4 | 230 | 0.9931 | 0.9998 | 0.9996 | 0.9987 | 0.9996 | 0.9892 | 0.9969 | 0.9979 | 0.9979 | 0.9742 |
| G3 | 230 | 0.9969 | 1.0015 | 1.0011 | 1.0018 | 1.0015 | 0.9933 | 0.9971 | 0.9512 | 0.9982 | 1.0026 |
| | 132 | 0.9883 | 0.9952 | 0.9958 | 0.9939 | 0.9959 | 0.9914 | 0.9984 | 0.9754 | 0.9969 | 1.0010 |
| S1 | 230 | 0.9881 | 0.9937 | 0.9939 | 0.9931 | 0.9752 | 0.9946 | 0.9978 | 0.9984 | 0.9985 | 0.9998 |
| | 63 | 0.9671 | 0.9753 | 0.9752 | 0.9745 | 0.9936 | 0.9902 | 0.9947 | 0.9955 | 0.9955 | 0.9852 |
| S4 | 230 | 0.9837 | 0.9942 | 0.9939 | 0.9958 | 0.9942 | 0.9782 | 0.9892 | 0.9911 | 0.997 | 0.9951 |
| | 63 | 0.9670 | 0.9821 | 0.9818 | 0.9886 | 0.9825 | 0.969 | 0.9842 | 0.9859 | 0.994 | 0.9888 |
| S5 | 230 | 0.9928 | 0.9985 | 0.9983 | 1.0008 | 0.9986 | 0.9851 | 0.9906 | 0.9716 | 0.9708 | 0.9968 |
| | 63 | 0.9896 | 0.9967 | 0.9962 | 1.0011 | 0.9967 | 0.9812 | 0.9874 | 0.9676 | 0.9689 | 0.9949 |
| S6 | 230 | 0.9888 | 1.0005 | 1.0006 | 0.999 | 1.0009 | 0.9806 | 0.9937 | 0.9953 | 0.9986 | 1 |
| | 63 | 0.9642 | 1 | 1 | 0.9866 | 1 | 0.9644 | 1 | 1 | 0.9907 | 1 |
| S7 | 230 | 0.9766 | 0.9916 | 0.9908 | 0.9853 | 0.9913 | 0.9685 | 0.9886 | 0.9895 | 0.9834 | 0.9856 |
| | 63 | 0.9671 | 1 | 1 | 0.9792 | 1 | 0.9521 | 1 | 1 | 0.9701 | 1 |
| S3 | 230 | 0.9894 | 0.9974 | 0.9973 | 0.9962 | 0.9971 | 0.9852 | 0.9938 | 0.9952 | 0.9954 | 0.9762 |
| | 63 | 0.9743 | 0.9875 | 0.9867 | 0.9833 | 0.9878 | 0.9713 | 0.987 | 0.9888 | 0.9844 | 0.9700 |
| S8 | 230 | 0.9819 | 0.9925 | 0.992 | 0.9933 | 0.9923 | 0.9760 | 0.9871 | 0.9887 | 0.9934 | 0.9888 |
| | 63 | 0.9668 | 0.9804 | 0.9801 | 0.9845 | 0.9803 | 0.9655 | 0.9795 | 0.98 | 0.9887 | 0.9807 |
| S9 | 230 | 0.9866 | 0.9973 | 0.997 | 0.9984 | 0.9972 | 0.9794 | 0.9908 | 0.9928 | 0.9977 | 0.9938 |
| | 132 | 0.9720 | 0.9843 | 0.9839 | 0.9817 | 0.9842 | 0.9789 | 0.99 | 0.9763 | 0.9897 | 0.9919 |
| | 63 | 0.9365 | 0.9882 | 0.9869 | 1 | 0.987 | 0.9717 | 0.9967 | 0.9854 | 1 | 0.9899 |
| S10 | 230 | 0.9896 | 0.997 | 0.9966 | 0.9998 | 0.997 | 0.9822 | 0.9897 | 0.9787 | 0.9811 | 0.9976 |
| | 63 | 0.9577 | 0.9878 | 0.9874 | 0.9964 | 0.9878 | 0.9714 | 0.9802 | 0.9684 | 0.9828 | 0.9885 |
| S2 | 230 | 0.9833 | 0.9942 | 0.9941 | 0.9932 | 0.994 | 0.9869 | 0.9952 | 0.9964 | 0.9964 | 0.9809 |
| | 63 | 0.9694 | 0.9995 | 0.9892 | 0.9882 | 0.9895 | 0.9842 | 0.9931 | 0.9945 | 0.9941 | 0.978 |
| S13 | 230 | 0.9863 | 0.9947 | 0.9944 | 0.9995 | 0.9948 | 0.9796 | 0.9882 | 0.9800 | 0.9886 | 0.996 |
| | 63 | 0.9747 | 0.9859 | 0.9855 | 1 | 0.9858 | 0.9684 | 0.9792 | 0.9709 | 1 | 0.9870 |
| S12 | 230 | 0.9815 | 0.9928 | 0.9924 | 0.9928 | 0.9925 | 0.9766 | 0.9883 | 0.9904 | 0.9932 | 0.9871 |
| | 63 | 0.9688 | 0.9867 | 0.9864 | 0.9852 | 0.9865 | 0.9641 | 0.9845 | 0.9856 | 0.9841 | 0.9837 |
| S11 | 230 | 0.9799 | 0.9903 | 0.9895 | 0.9903 | 0.9898 | 0.9726 | 0.9836 | 0.9848 | 0.9882 | 0.9796 |
| | 63 | 0.9732 | 0.9851 | 0.9851 | 0.9854 | 0.9846 | 0.954 | 0.9666 | 0.9678 | 0.9695 | 0.9619 |
| S14 | 230 | 0.9951 | 1.0004 | 1.0003 | 1.0019 | 1.0004 | 0.9909 | 0.9939 | 0.9468 | 0.9797 | 1 |
| | 63 | 0.9800 | 0.9852 | 0.9803 | 0.9874 | 0.9852 | 0.9752 | 0.9749 | 0.9267 | 0.961 | 0.984 |
| Average Voltage Deviation (%) | | 1.941 | 0.773 | 0.834 | 0.793 | 0.810 | 2.206 | 1.028 | 2.026 | 1.102 | 1.080 |

**Table 9. Optimal location and tap position of installed PSTs in scenario 2**

| PST No. | Line on which the PST is installed | Tap Position | | | | | | | | | | | |
|---|---|---|---|---|---|---|---|---|---|---|---|---|---|
| | | Normal Operation | | Contingency Operation (Contingency Number) | | | | | | | | | |
| | | Peak | Off-peak | Peak | | | | | Off-peak | | | | |
| | | | | 1 | 2 | 3 | 4 | 5 | 1 | 2 | 3 | 4 | 5 |
| 1 | G2-G3 | +1 | -2 | +3 | -1 | -1 | -2 | +3 | -6 | -6 | -2 | -2 | -2 |
| 2 | S14-G2 | +2 | +4 | +4 | -1 | -3 | +2 | -1 | +4 | +7 | +4 | +4 | +7 |
| 3 | G4-S3 | -1 | 0 | -1 | -1 | -2 | -2 | -2 | 0 | 0 | 0 | 0 | 0 |

**Table 10. Characteristics of installed PSTs in scenario 2**

| PST No. | Capacity of PST (MVA) | Tap range (phase shift of each tap is 2.5$^O$ ) |
|---|---|---|
| 1 | 149.5 | ±6 |
| 2 | 464.8 | ±7 |
| 3 | 134.7 | ±2 |

**Table 11. Optimal location and injected reactive power of installed SVCs in scenario 2**

| SVC No. | Substation on which the SVC is installed | Injected Reactive Power (MVAr) | | | | | | | | | | | |
|---|---|---|---|---|---|---|---|---|---|---|---|---|---|
| | | Normal Operation | | Contingency Operation (Contingency Number) | | | | | | | | | |
| | | Peak | Off-peak | Peak | | | | | Off-peak | | | | |
| | | | | 1 | 2 | 3 | 4 | 5 | 1 | 2 | 3 | 4 | 5 |
| 1 | S7 | 61.8 | 100.7 | 56.6 | 113.9 | 69.9 | 63.8 | 56.8 | 99 | 100.8 | 100.7 | 100.6 | 100.3 |
| 2 | S6 | 131.6 | 121 | 208.9 | 121.2 | 146.6 | 134.9 | 136.2 | 120.3 | 121.3 | 121 | 121 | 115 |

**Table 12. Characteristics of installed SVCs in scenario 2**

| SVC No. | Capacity of SVC (MVAr) |
|---------|------------------------|
| 1 | 113.9 |
| 2 | 208.9 |

**Table 13. Optimal location and tap position of installed PSTs in scenario 3**

| PST No. | Line on which the PST is installed | Tap Position | | | | | | | | | | | |
|---------|-----------------------------------|--------------|---|---|---|---|---|---|---|---|---|---|---|
| | | Normal Operation | | Contingency Operation (Contingency Number) | | | | | | | | | |
| | | Peak | Off-peak | Peak | | | | | Off-peak | | | |
| | | | | 1 | 2 | 3 | 4 | 5 | 1 | 2 | 3 | 4 |
| 1 | S3-Siadat | +2 | +2 | 0 | 0 | -3 | -2 | +4 | -2 | +3 | +2 | -1 |
| 2 | Gilan-Loshan | -2 | +1 | 0 | -2 | -2 | -2 | -2 | +4 | +2 | +5 | +1 |

**Table 14. Characteristics of installed PSTs in scenario 3**

| PST No. | Capacity of PST (MVA) | Tap range (phase shift of each tap is 2.5$^O$ ) |
|---------|----------------------|------------------------------------------------|
| 1 | 134 | ±4 |
| 2 | 167 | ±5 |

**Table 15. Optimal location and injected reactive power of installed SVCs in scenario 3**

| SVC No. | Substation on which the SVC is installed | Injected Reactive Power (MVAr) | | | | | | | | | | | |
|---------|------------------------------------------|-------------------------------|---|---|---|---|---|---|---|---|---|---|---|
| | | Normal Operation | | Contingency Operation (Contingency Number) | | | | | | | | | |
| | | Peak | Off-peak | Peak | | | | | Off-peak | | | |
| | | | | 1 | 2 | 3 | 4 | 5 | 1 | 2 | 3 | 4 |
| 1 | S9 | 139.7 | 91.6 | 199.6 | 146.9 | 169.3 | 142.2 | 143.9 | 91.4 | 85.7 | 105.1 | 92.2 |
| 2 | S13 | 63.8 | 145.5 | 60.6 | 60.2 | 65.4 | 64.7 | 65.6 | 199 | 223 | 120.7 | 162.9 |

**Table 16. Characteristics of installed SVCs in scenario 3**

| SVC No. | Capacity of SVC (MVAr) |
|---------|------------------------|
| 1 | 199.6 |
| 2 | 223 |

**Table 17. Optimal location and tap position of installed PSTs in scenario 4**

| PST No. | Line on which the PST is installed | Tap Position | | | | | | | | | |
|---------|-----------------------------------|--------------|---|---|---|---|---|---|---|---|---|
| | | Normal Operation | | Contingency Operation (Contingency Number) | | | | | | | |
| | | Peak | Off-peak | Peak | | | | Off-peak | | | |
| | | | | 1 | 2 | 3 | 4 | 1 | 2 | 3 | 4 |
| 1 | S3-S9 | +1 | -2 | +2 | +1 | +2 | +1 | -3 | -1 | -3 | -1 |

**Table 18. Characteristics of installed PSTs in scenario 4**

| PST No. | Capacity of PST (MVA) | Tap range (phase shift of each tap is 2.5$^O$ ) |
|---------|----------------------|------------------------------------------------|
| 1 | 100.88 | ±3 |

**Table 19. Optimal location and injected reactive power of installed SVCs in scenario 4**

| SVC No. | Substation on which the SVC is installed | Injected Reactive Power (MVAr) | | | | | | | | | |
|---------|------------------------------------------|-------------------------------|---|---|---|---|---|---|---|---|---|
| | | Normal Operation | | Contingency Operation (Contingency Number) | | | | | | | |
| | | Peak | Off-peak | Peak | | | | Off-peak | | | |
| | | | | 1 | 2 | 3 | 4 | 1 | 2 | 3 | 4 |
| 1 | S7 | 63 | 124.4 | 58.5 | 70.4 | 65.2 | 66.3 | 122.1 | 127.4 | 197.5 | 127.5 |
| 2 | S6 | 130.6 | 96.6 | 209.3 | 143.5 | 133.4 | 133.2 | 171.2 | 98.5 | 89.3 | 103 |

**Table 20. Characteristics of installed SVCs in scenario 4**

| SVC No. | Capacity of SVC (MVAr) |
|---------|------------------------|
| 1 | 197.5 |
| 2 | 209.3 |

(a)



(b)
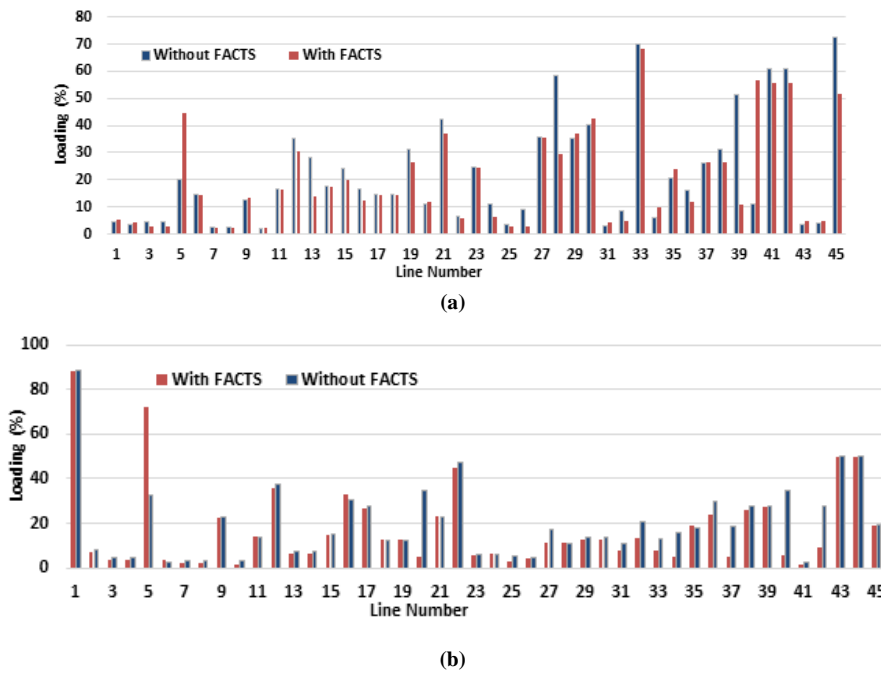
**Fig. 10. Transmission lines' loading in scenario 1, (a): Peak (b):Off-peak**



(a)



(b)
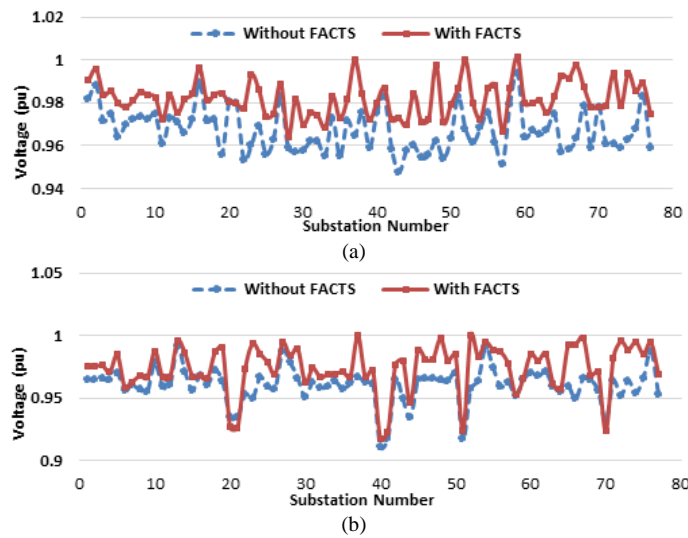
**Fig. 11. Voltage magnitude of sub-transmission level buses before and after installation of FACTS devices for scenario 2 (a): peak (b): off-peak**
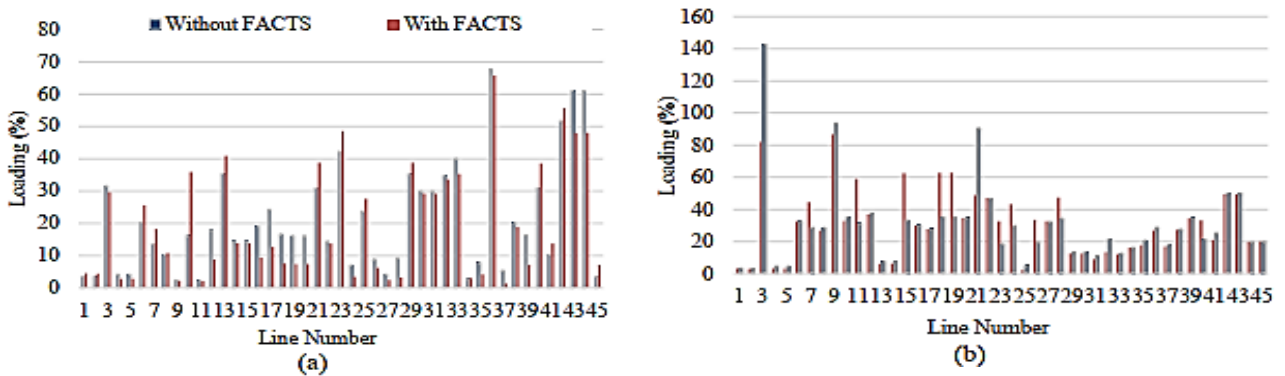


**Fig. 12. Transmission lines' loading in scenario 2, (a): Peak (b):Off-peak**
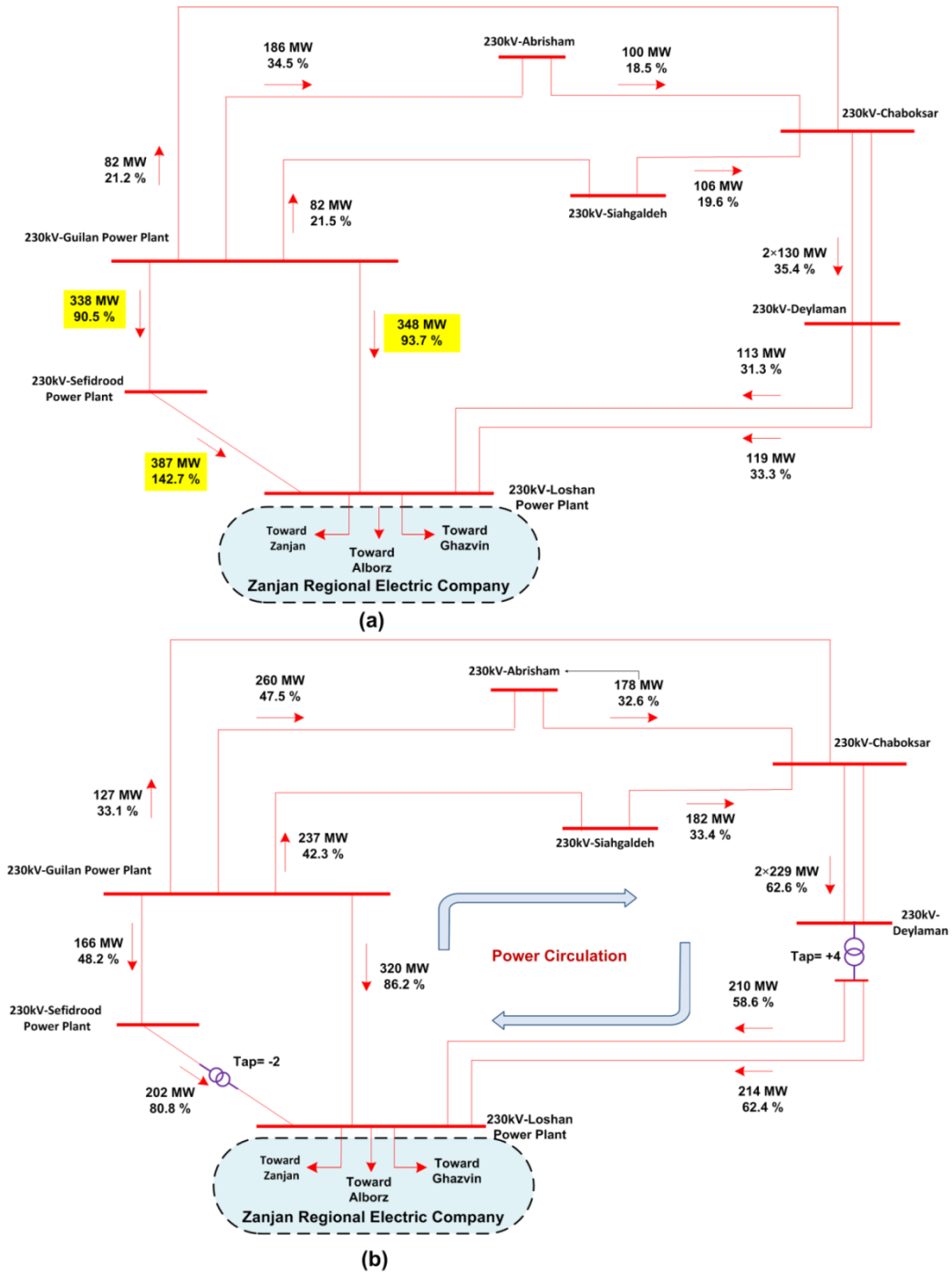
**Fig. 13. Loading of transmission lines in south part of the network in off-peak condition of scenario 2, (a): without FACTS (b): with FACTS**
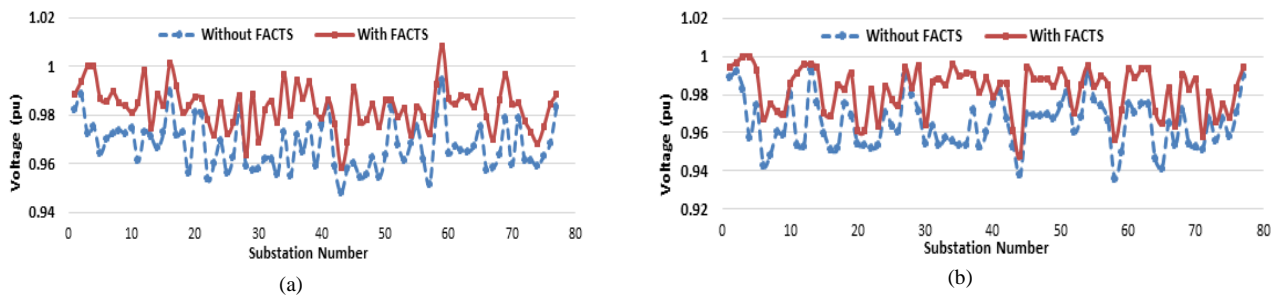


**Fig. 14. Voltage magnitude of sub-transmission level buses before and after installation of FACTS devices for scenario 3 (a): peak (b): off-peak**

(a)                                                                                      (b)
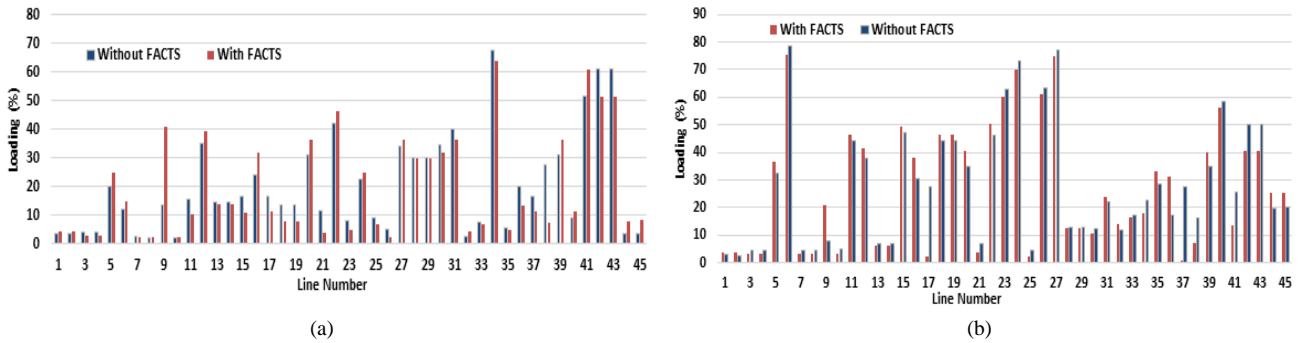
**Fig. 15. Transmission lines' loading in scenario 3, (a): Peak (b):Off-Peak**
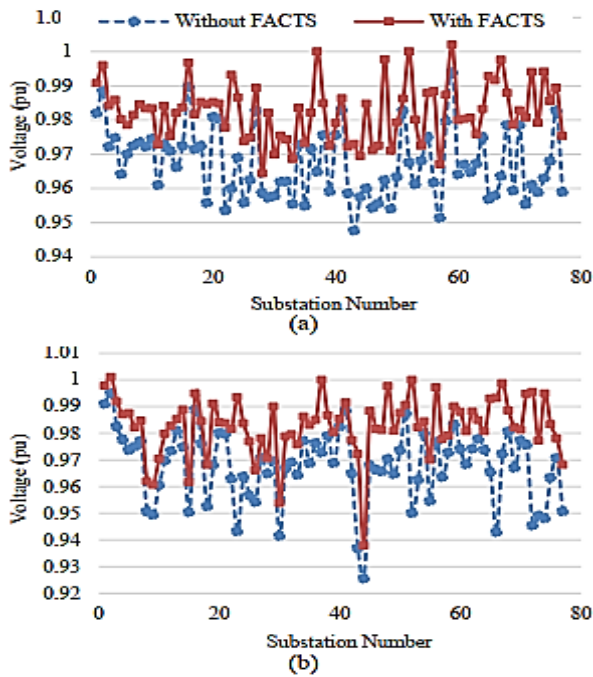


**Fig. 16: Voltage magnitude of sub-transmission level buses before and after installation of FACTS devices for scenario 4 (a): peak (b): off-peak**

### 5.4. Convergence trend of DPSO

To see the performance of DPSO, the convergence curve of the algorithm has been depicted in Fig. 18 for scenario 2 for different number of SVC and PST. In all three cases, the number of particles and iterations are 20 and 800, respectively. Since the objective function is normalized, the starting point is from 2; on this basis, the more the number of FACTS devices, the lower the value of objective function, which means reduction of lines loading and voltage deviation of buses. To evaluate the efficiency of employed DPSO algorithm, the problem is also programmed and executed by the genetic algorithm (GA) with 20 chromosomes. Table 21 shows the value of objective function for the two algorithms in scenario 2. Also, in Fig. 18, the convergence trend of these algorithms can be compared. As it is observed, the values of objective function in the two algorithms are near together. However, DPSO has

yield better values for the objective function. In addition, the convergence behavior of DPSO is better than GA, so that it finds the optimal solution in relatively lower number of iterations. Also, it can be said that, when the number of variables increases (the green curve in Fig. 18, i.e. 2PST+2SVC case), the efficiency of DPSO is more clearly demonstrated.
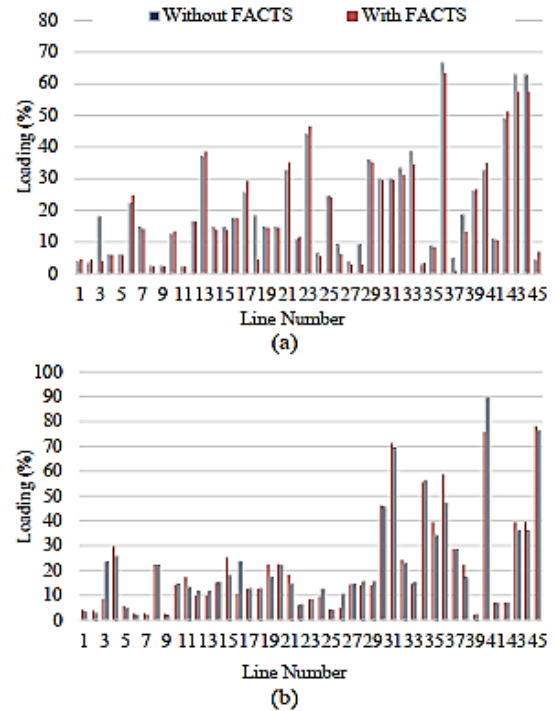


**Fig. 17: Transmission lines' loading in scenario 4, (a): Peak (b):Off-peak**
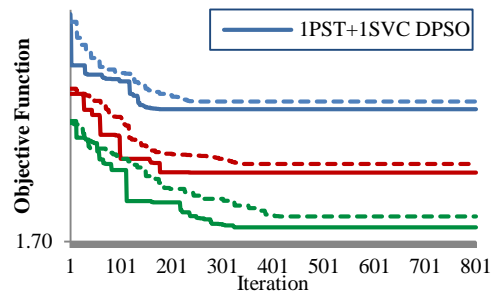


**Fig. 18. Convergence trend of DPSO compared with GA in scenario 2**

**Table 21. Comparing the of objective function using GA and DPSO algorithms in scenario 2**

| Algorithm | Number of PST and SVC | | |
|-----------|----------|----------|----------|
|           | 1PST+1SVC | 1PST+2SVC | 2PST+2SVC |
| GA        | 1.8330   | 1.7737   | 1.7237   |
| DPSO      | 1.8256   | 1.7655   | 1.7134   |

## 5.5. Evaluating the effect of FACTS devices in contingency and dynamic conditions

### 5.5.1. Contingency

As mentioned before, in addition to normal operation, the algorithm also tries to alleviate the congestion in contingency conditions. To investigate this capability, the outage of a 230kV line connecting S6 substation to G1 power plant is considered. As Fig. 19a shows, by outage of this line, the line between G1 power plant and S9 substation is overloaded by 118%. By installing a PST on the line S9-S3 and adjusting its tap position to -3, the loading of G1-S9 line is decreased to 98%, and the congestion is resolved (Fig. 19b). The voltage magnitude and angle of buses have been shown in Fig.

19 to see the effect of PST on the power flow of the network. It should be noted that, because of the page limitation, just some part of the network has been shown in Fig. 19.

### 5.5.2. Dynamic performance

The performance of the allocated FACTS devices in Gilan network can be evaluated by dynamic simulations. As an example of network dynamic performance is studied in this part. A three-phase short circuit fault is applied to 230kV line of G1-S6 in second 2, and after 0.1 seconds, the fault is cleared by the outage of this line using the circuit breakers located at two endings of this line. This event was one of the contingencies of scenario 1 given in Table 3. The variations of voltage magnitude of S6 substation during this event has been shown in Fig. 20. As seen, the SVC unit located in S6 substation has effectively restored the voltage to 1p.u. while it was drastically dropped without the presence of SVC.
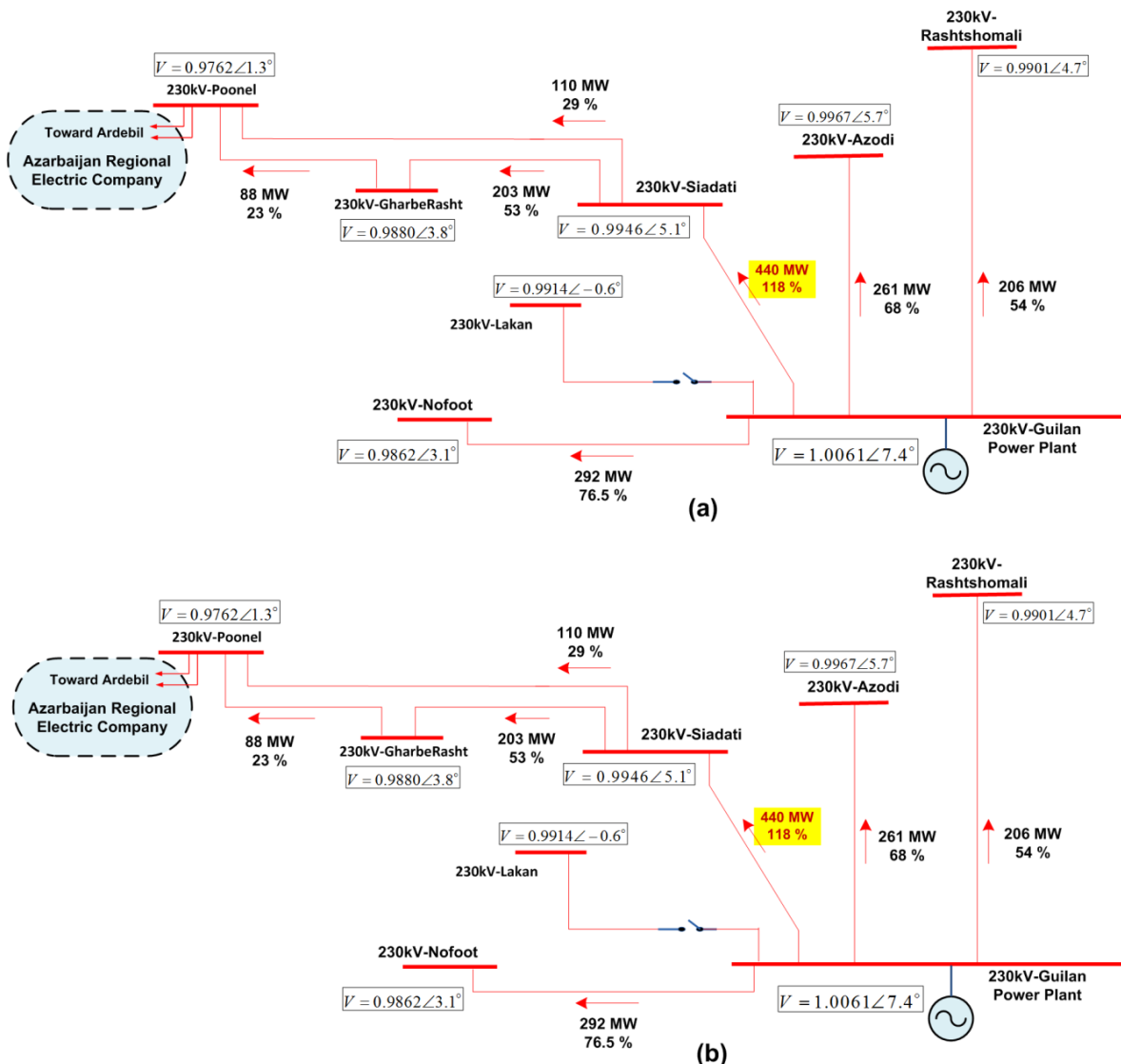


**Fig.19. Loading of transmission lines in outage of S6-G1 230-kV line in off-peak condition of scenario 4, (a): without FACTS (b) with FACTS**
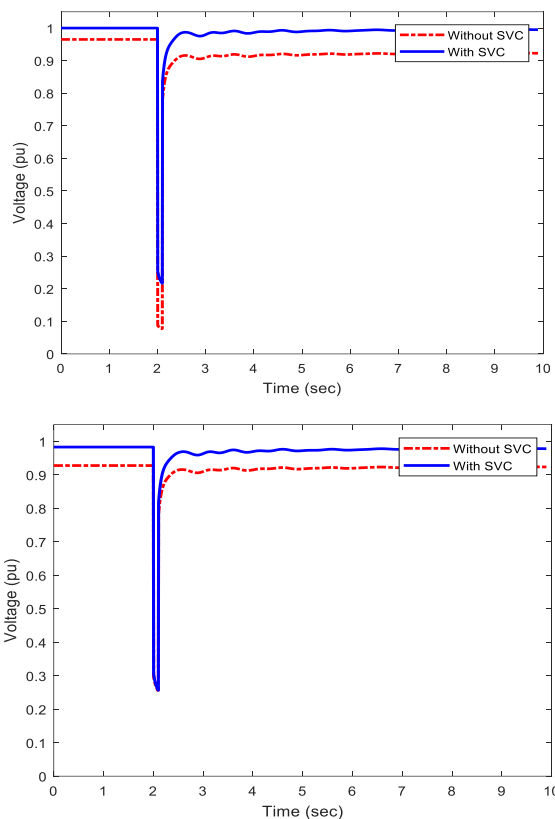
**Fig. 20. Voltage variations of S6 substation by the outage of G1-S6 230-kV line in peak condition of scenario 1, (a): 63kV bus, (b) 230kV bus**

### 5.6. Discussion on the results

The Gilan's power grid is a compact network, meaning that its load is high relative to the geographical area. In this network, in the horizon year (2026), there are four power plants with the nominal capacity of 2568MW; the peak and off-peak loads are 2535MW and 1244MW, respectively. The major concern in the peak condition is that there is high voltage drop in some substations. On the other hand, in off-peak condition, as the power generation is almost 1200MW greater than the load, the surplus power is exported to the neighboring networks through the transmission lines, and this leads to congestion in the related routes. In this regard, two elements of FACTS devices are supportive in settling of these two problems: SVC for improving the voltage profile, and PST to alleviate the congestion of lines. Based on the four considered scenarios, it was seen that two SVCs are required for the compensation of voltage and reactive power; and also, three PST units are needed for the congestion management: one in south part of the network to control the power flow when exchanging power with the southern networks, one in east, and one in the west part. By these three PSTs, the overloading problem is settled down both in the normal and

contingency conditions. It is worth mentioning that an economic study is also required to compare the cost installing FACTS devices with the cost of network upgrade through traditional solutions, i.e., installation of substations and lines. This study has been implemented by the authors, and it showed that the FACTS installation is more economical than the traditional solution; however, because of the page limitation, this comparison has not been reported here. It also should be noted that due to special geographical conditions of Gilan network, such as soil looseness and forest areas, construction of new substations and transmission lines is highly restricted. As the final conclusion, we can say that the FACTS installation is a better choice for the Gilan electric grid whether from technical, economical, or environmental aspects.

### 6. CONCLUSION

In this paper, a DIgSILENT-based DPSO algorithm was employed to improve the technical parameters of a real-case network located in north of Iran using FACTS devices. The superiority of the conducted approach over the existing methods is its applicability to practical real-world systems and its user-friendly environment for the engineers. The SVC and PST as two elements of FACTS family are employed to manage the power flow and improve the voltage profile. By optimal allocation of SVC and PST and tap setting of PST units, the voltage of substations is regulated to appropriate values, the congestion of transmission lines in normal and contingency conditions is resolved, and no generation block is occurred either in normal or contingency cases. Table 8 showed that the FACTS devises have decreased average voltage deviation (AVD) of buses in all scenarios of peak and off-peak conditions. The AVD in peak condition without the use of FACTS devices was 1.941% which it is decreased to 0.773, 0.834, 0.793, and 0.81% respectively for scenarios 1, 2, 3, and 4. Also, the AVD in off-peak condition without the use of FACTS devices was 2.226% which it is decreased to 1.0228, 2.026, 1.102, and 1.08% respectively for scenarios 1- 4. Also, in all scenarios, the average loading of transmission and sub-transmission lines have been decreased. As the calculations are performed in DIgSILENT software, the proposed methodology can be easily extended to other studies such as optimal transmission switching (TS), transmission expansion planning (TEP), optimal power flow (OPF), optimal adjustment of generating units' voltage set-point, and etc. Also, other parameters as such as power loss and reactive power flow minimization can be considered as the objective function.

**REFERENCES**

[1] R. Hemmati, R. Hooshmand and A. Khodabakhshian, "Market based transmission expansion and reactive power planning with consideration of wind and load uncertainties", *Renewable Sustainable Energy Rev*., vol. 29, pp. 1-10, 2014.

[2] T. Kishore and S. Singal, "Optimal economic planning of power transmission lines: a review", *Renewable Sustainable Energy Rev*., vol. 39, pp. 949-974, 2014.

[3] R. Shah, N. Mithulananthan, R. Bansal and V. Ramachandaramurthy, "A review of key power system stability challenges for large-scale PV integration", *Renewable Sustainable Energy Rev*., vol. 41, pp.1423-1436, 2015.

[4] K. Verma, S. Singh and H. Gupta, "Location of unified power flow controller for congestion management", *Elect. Power Syst. Res*., vol. 58, pp. 89-96, 2001.

[5] J. Singh, S. Singh and S. Srivastava, "An approach for optimal placement of static VAr compensators based on reactive power spot price", *IEEE Trans. Power Syst*., vol. 22, pp. 2021-2029, 2007.

[6] N. Hingoran, L. Gyugyi and M. Hawary, "Understanding FACTS: concepts and technology of flexible AC transmission systems", *IEEE press*, vol. 1, 2000.

[7] T. Nireekshana, G. Kesava and S. Siva, "Enhancement of ATC with FACTS devices using Real-code genetic algorithm", *Elect. Power Energy Syst.,* vol. 43, pp. 1276-1284, 2012.

[8] E. Ali and S. AbdElazim, "TCSC damping controller design based on bacteria foraging optimization algorithm for a multi-machine power system", *Elect. Power Energy Syst*., vol. 37, pp.23-30, 2012.

[9] R. Sirjani, A. Mohamed and H. Shareef, "Optimal allocation of shunt var compensators in power systems using a novel global harmony search algorithm", *Elect. Power Energy Syst.* vol. 43, pp. 562-572, 2012,

[10] D. Mondal, A. Chakrabarti and A. Sengupta, "Optimal placement and parameter setting of SVC and TCSC using PSO to mitigate small signal stability problem", *Electr. Power Energy Syst*., vol. 42, pp. 334-340, 2012.

[11] H. Shayeghi and M. Ghasemi, "FACTS devices allocation using a novel dedicated improved pso for optimal operation of power system", *J. Oper. Autom. Power Eng*., vol. 1, pp. 124-135, 2013.

[12] R. Kazemzadeh, M. Moazen, R. Ajabi-Farshbaf and M. Vatanpour, "STATCOM optimal allocation in transmission grids considering contingency analysis in OPF using BF-PSO algorithm", *J. Oper. Autom. Power Eng*., vol. 1, pp. 1-11, 2013.

[13] S. Dutta, P. Roy and D. Nandi, "Optimal location of UPFC controller in transmission network using hybrid chemical reaction optimization algorithm", *Electr. Power Energy Syst*., vol. 64, pp. 194-211, 2015.

[14] J. Sarker and S. Goswami, "Solution of multiple UPFC placement problems using gravitational search algorithm", *Electr. Power Energy Syst*., vol. 55, pp. 531-541, 2014.

[15] A. Rezaee, "Brainstorm optimization algorithm (BSOA): An efficient algorithm for finding optimal location and setting of FACTS devices in electric power systems", *Electr. Power Energy Syst*., vol. 69, pp. 48-57, 2015.

[16] C. Duan, W. Fang, L. Jiang and Sh. Niu, "FACTS devices allocation via sparse optimization", *IEEE Trans. Power Syst*., vol. 31. pp. 1308-1319, 2016.

[17] A. Elmitwally, A. Eladl and J. Morrow, "Long-term economic model for allocation of FACTS devices in restructured power systems integrating wind generation", *IET Gener. Tranms. Distrib*., vol. 10, pp. 16-30, 2016.

[18] X. Zhang and et. al., "Optimal allocation of series facts devices under high penetration of wind power within a market environment", *IEEE Trans. Power Syst.,*vol. 33, pp. 6206-6217, 2018.

[19] X. Zhang, K. Tomsovic and A. Dimitrovski, "Optimal allocation of series FACTS devices in large-scale systems", *IET Gener. Transm. Distrib*., vol. 12, pp. 1889-1896, 2018.

[20] K. Sen and M. Sen, "Introduction to FACTS controllers: theory, modeling and applications", *Wiley and IEEE Press*, USA, 2009.

[21] M. Eremia, C. Liu and A. Edris, "Advanced solutions in power systems: HVDC, FACTS, and Artificial Intelligence", *IEEE Press and Wiley*, USA, 2016.

[22] M. Eremia and M. Sphahidehpour, "Handbook of electrical power system dynamics: modeling, stability and control", *IEEE Press* and Wiley, USA, 2013.

[23] J. Gholinezhad, R. Noroozian and A. Bagheri, "Optimal capacitor allocation in radial distribution networks for annual costs minimization using hybrid pso and sequential power loss index based method", *J. Oper. Autom. Power Eng*., vol. 5, pp. 51-60, 2017.

[24] R. Eberhart and J. Kennedy, "A new optimizer using particle swarm theory", *Proc. Sixth Int. Symp. Micro Mach. Hum. Sci.,* Japan, pp. 39-43, 1995.

[25] Y. Jin, H. Cheng, J. Yan and L. Zhang, "New discrete method for particle swarm optimization and its application in transmission network expansion planning", *Electr. Power Syst. Res*., vol. 77, pp. 227-233, 2007.

[26] M. Clerc and J. Kennedy, "The particle swarm-explosion, stability, and convergence in a multidimensional complex space", *IEEE Trans. Evol. Comput.,* vol. 6, pp. 58-73, 2002.

[27] A. Nickabadi, M. Ebadzadeh and R. Safabakhsh, "A novel particle swarm optimization algorithm with adaptive inertia weight", *Appl. Soft Comput.*, vol. 11, pp. 3658-3670, 2011.

[28] Guilan Regional Electric Company at:https://www.gilrec.co.ir.

[29] P. Kundur, "Power system stability and control", *McGraw-Hill Education*; 1st edition, 1994.